ELSEVIER

Solid State Ionics 99 (1997) 15–22

SOLID STATE IONICS

Chemical diffusion and oxygen exchange of $La_{0.6}Sr_{0.4}Co_{0.6}Fe_{0.4}O_{3-\delta}$

J.E. ten Elshof*, M.H.R. Lankhorst, H.J.M. Bouwmeester

Laboratory for Inorganic Materials Science, University of Twente, P.O. Box 217, 7500 AE Enschede, The Netherlands

Received 26 February 1997; accepted 14 April 1997

Abstract

The transport parameters of $La_{0.6}Sr_{0.4}Co_{0.6}Fe_{0.4}O_{3-\delta}$ were determined by electrical conductivity relaxation and high temperature coulometric titration experiments. The experimental response curves were analyzed in the frequency domain. The results obtained by both methods were in good agreement. The chemical diffusion coefficients measured at temperatures of 923–1255 K and oxygen partial pressures of 0.03–1 bar O_2, vary between 10^{-6}–5×10^{-5} $cm^2\,s^{-1}$. The experimental activation energies are in the range 95–117 kJ mol^{-1}. At oxygen partial pressures below 0.03 bar O_2 the re-equilibration process is completely governed by the rate of oxygen exchange at the interface. The surface exchange coefficients were determined by conductivity relaxation experiments at temperatures of 1000–1285 K and oxygen pressures of 10^{-4}–0.1 bar O_2. The activation energy is about 60–70 kJ mol^{-1}. The exchange coefficients are almost proportional to the oxygen pressure. Treatment of the surface in a nitric acid solution for several hours increases the surface exchange rates by factors of 3–5.

Keywords: Mixed conducting oxide; Perovskite; Lanthanum strontium cobalt iron oxide; Chemical diffusion; Oxygen exchange

1. Introduction

Knowledge of the relevant transport parameters of solid oxides is of fundamental importance in the development of high temperature solid state electrochemical devices. Several experimental techniques have already been employed in the study of oxygen transport through perovskite-type oxides, such as isotopic exchange analysis [1–3], transient thermogravimetry [4], oxygen coulometric titration [5–7] and electrical conductivity relaxation [8–10].

Transient methods are based on the principle of subjecting an oxide sample to a sudden change of the oxygen chemical potential of the ambient atmosphere and monitoring the rate at which the specimen proceeds to equilibrium. The transient response is commonly analyzed in the time domain under the assumption that chemical diffusion is the only rate-determining factor in the re-equilibration process [5,11]. In general, however, the rate of re-equilibration may also be affected by slow interfacial exchange, gas phase diffusion and, in the case of oxygen coulometric titration, polarization losses over electrical wiring and contacts.

These contributions can be discriminated from chemical diffusion by analysing the experimental data in the frequency domain. This approach has been followed in recent studies on chemical diffusion

*Corresponding author.

PII S0167-2738(97)00263-4

in $La_{0.8}Sr_{0.2}CoO_{3-\delta}$ [7] and $La_{1-x}Sr_xFeO_{3-\delta}$ ($x = 0.1$, 0.4) [12]. In the present paper the chemical diffusion and surface exchange coefficients of $La_{0.6}Sr_{0.4}Co_{0.6}Fe_{0.4}O_{3-\delta}$ are determined. Both electrical conductivity relaxation and oxygen coulometric titration are applied. The analysis of transient data is performed in the frequency domain and the results obtained with the two techniques are compared.

2. Theory

A solid oxide body in chemical and thermal equilibrium with the surrounding atmosphere has a uniform bulk concentration of oxygen $c_b(x,y,z,t)$ equal to c_0. At $t=0$, the oxygen activity in the ambient atmosphere is changed stepwise to a value corresponding to a new equilibrium concentration c_∞ in the solid. Chemical diffusion allows the sample to adapt its stoichiometry to c_∞. The concentration at any point (x,y,z) in the bulk at time $t>0$ can be calculated from the solution of Fick's second law

$$\frac{\partial c(x,y,z,t)}{\partial t} = \tilde{D}\nabla^2 c(x,y,z,t). \tag{1}$$

The bulk concentration is expressed relative to its initial concentration: $c(x,y,z,t)=c_b(x,y,z,t)-c_0$. $\tilde{D}$ is the chemical diffusion coefficient. A boundary condition appropriate for both types of measurements performed here is $c(x,y,z,0)=0$. Their respective cases are discussed below.

2.1. Electrical conductivity relaxation

The electrical conductivity relaxation technique is based on the principle that a change of the nonstoichiometry δ of a specimen is reflected in a change of the apparent macroscopic conductivity σ_{app}. The relative change of conductivity σ_{app}^{rel} after a stepwise change of the ambient oxygen pressure is related to the mass change m of the specimen via [13]

$$\sigma_{app}^{rel}(t) = \frac{\sigma_{app}(t)-\sigma_{app}(0)}{\sigma_{app}(\infty)-\sigma_{app}(0)} = \frac{m(t)}{m(\infty)}, \tag{2}$$

provided that the conductivity is measured in a direction perpendicular to the direction in which oxygen diffusion occurs in the sample. Even when electrical conductivity and departure from stoichiometry are not linearly related, this relationship can still be applied as long as there is no extremum in the electrical conductivity within the re-equilibration step [11].

The geometry and dimensions of the oxide samples used in the present electrical relaxation experiments were selected such that diffusion occurs in one direction (z) only. Considering diffusion in a sheet of thickness L ($-\frac{1}{2}L \le z \le \frac{1}{2}L$), the boundary conditions for the interfaces are $-\tilde{D}(\partial c(z,t)/\partial z)_{z=\pm L/2} = \mp K_{ex}(\Delta c - c(\pm\frac{1}{2}L,t))$, where K_{ex} is the apparent surface exchange coefficient and $\Delta c = c_\infty - c_0$. That is, the oxide surface is assumed not to equilibrate immediately with the newly imposed ambient atmosphere, but equilibration is described by a linear rate law. Eq. (1) is readily solved in the Laplace domain [12], yielding

$$\overline{c(z,s)} = \frac{\Delta c}{s}\left(1+\frac{k\tilde{D}}{K_{ex}}\tanh(\tfrac{1}{2}kL)\right)^{-1}\frac{\cosh(kz)}{\cosh(\frac{1}{2}kL)}, \tag{3}$$

with $\overline{c(z,s)}$ the Laplace transform of $c(z,t)$, and $k=\sqrt{s/\tilde{D}}$. The total mass change $\overline{m(s)}$ in the frequency domain is obtained by integration of Eq. (3) over the specimen volume. An impedance representation $\overline{Z(s)}$ of the theoretical solution can be given [12]

$$\overline{Z(s)} = \frac{1}{s^2}\frac{m(\infty)}{\overline{m(s)}} = \frac{L}{2K_{ex}} + \sqrt{\frac{L^2}{4\tilde{D}s}}\coth(\tfrac{1}{2}kL) = R_s + T(s). \tag{4}$$

Hence, the impedance can be described by a serial arrangement of a resistance R_s, associated with the limited oxygen exchange rate at the interface and an element $T(s)$, describing the finite length diffusion in the sample.

2.2. Coulometric titration

In coulometric titration measurements the sample is enclosed in an isolated compartment. Two of the compartment walls are oxygen-conducting solid electrolytes with identical metallic electrodes attached to both sides, and in contact on opposite sides with the atmosphere inside the cell and a reference gas,

respectively. The oxygen pressure inside the cell is controlled by imposing an EMF across one of the electrolytes. After a sudden potentiostatic change by a value ΔEMF, the gas/solid system inside the cell re-equilibrates by electrochemical pumping of oxygen through the second electrolyte wall. The electrical decay current $I(t)$ through this electrolyte is monitored. Upon neglecting the gas phase capacity for oxygen, this current is equal to the electrical current through the sample interfaces.

The samples used in the present experiments are disk-shaped (radius R, thickness L). Due to the complicated mathematics involved, the diffusion equation is solved under the simplifying assumption that the surface reaction is very fast. Using cylindrical coordinates ($-\frac{1}{2}L \le z \le \frac{1}{2}L$; $0 \le r \le R$), the boundary conditions are $c(\pm\frac{1}{2}L,r,t) = c(z,R,t) = \Delta c$ and $(\partial c(z,r,t)/\partial r)_{r=0} = 0$. The solution to Fick's second law is [14]

$$\overline{c(z,r,s)} = \frac{\Delta c}{s}\left(1 - \sum_{i=1}^{\infty}\sum_{n=1}^{\infty}\left(\frac{2J_0(\alpha_i r/R)}{\alpha_i J_1(\alpha_i)}\right) \times\left(\frac{-4\cos((2n-1)\pi z/L)}{(-1)^n(2n-1)\pi}\right) \times \frac{s\tau}{s\tau + \alpha_i^2/\alpha + (2n-1)^2\pi^2/\beta}\right), \quad (5)$$

where $\alpha = R^2/(R^2+L^2)$, $\beta = L^2/(R^2+L^2)$, and $\tau = (R^2+L^2)/\tilde{D}$. J_0 and J_1 are 0^{th} and 1^{st} order Bessel functions, respectively, and α_i is the i^{th} value for which $J_0(\alpha_i) = 0$. The frequency transform of the electrical current, $\overline{I(s)}$, associated with transport of O^{2-} through the sample interfaces, can be calculated from Fick's first law using Eq. (5). The impedance of the sample due to diffusion, defined by $\overline{T(s)} = \overline{\Delta EMF}/\overline{I(s)}$, is [14]

$$\overline{T(s)} = \left(\frac{\Delta EMF}{\Delta Q}\right)\left(\frac{\alpha\beta\tau}{32}\right)\left(\sum_{i=1}^{\infty}\sum_{n=1}^{\infty}\left(\frac{\alpha}{\alpha_i^2} + \frac{\beta}{(2n-1)^2\pi^2}\right) \times\left(\frac{s\tau}{s\tau + \alpha_i^2/\alpha + (2n-1)^2\pi^2/\beta}\right)\right)^{-1}, \quad (6)$$

where $\Delta Q = -2eR^2L\Delta c$ (e is the elementary electron charge) is the total electrical charge pumped through the electrolyte in the course of re-equilibration.

3. Experimental

3.1. Sample preparation

The method of preparation of the samples has been described extensively elsewhere [15]. X-ray diffractometry (XRD) analysis indicated a single-phase perovskite-type oxide. The sample surfaces were polished with 1000 MESH SiC. The final samples had densities of 95–98% relative to theoretical. The sample for the coulometric titration experiment was disk-shaped ($R = 7.75$ mm, $L = 2.5$ mm). Rectangular samples of $27 \times 14 \times 0.51$ mm were used for the conductivity relaxation experiments. Some of the samples were given a treatment in a 2.5–5 M HNO_3 solution for 2–18 h [16], followed by ultrasonic cleaning in water and alcohol.

3.2. Electrical conductivity relaxation

Gold wires of 0.1 mm diameter were wound around the outer ends of the samples. The contact between wires and sample was provided by gold electrodes. The sample was placed in a quartz tube. A thermocouple to measure the temperature was positioned 3 mm above the sample. The quartz tube was flushed with oxygen diluted in nitrogen at atmospheric pressure. A second gas stream was vented. The oxygen concentrations in both streams, each with a flow of 100 ml min^{-1} (STP), were varied between 100 ppm and 100% and could be measured with an oxygen sensor. The flows leading to the sample and vent could be interchanged with a fast electrical four-way valve.

Oxygen pressure steps were performed in oxidizing and reducing direction, in which the oxygen partial pressure changed with a factor of 10 (at low temperature and high pressure) or less, typically a factor of about 3. The absence of mass transfer limitations in the gas phase was verified by variation of the total gas flow and the magnitude of the oxygen pressure step. Measurements were performed in the temperature range 1000–1285 K. To avoid mass

transfer limitations oxidation runs were only performed at a final oxygen concentration of 1% or more. Further details can be found elsewhere [12].

The specimen resistance was measured in a Wheatstone bridge using a lock-in amplifier. The experimental data $\sigma^{rel}_{app}(t)$ were transformed to an impedance representation $Z(j\omega) = -(\omega^2 \sigma^{rel}_{app}(j\omega))^{-1}$ and analyzed using Equivalent Circuit software [17] by fitting to a serial circuit consisting of a cotangent-hyperbolic function (T), representing a finite length diffusion element, and a resistance (R).

3.3. Coulometric titration experiments

Details regarding the equipment and experimental procedure can be found elsewhere [7,14]. The cell consisted of a YSZ crucible onto which a YSZ disk was sealed using a Pyrex glass ring. The internal volume of the cell was approximately 250 mm^3. Crucible and disk served as electrolytes and Pt-based electrodes were painted on opposite sides of both. The sealed cell containing the sample was placed in a quartz tube which was flushed with air.

Potentiostatic steps $\Delta EMF = 25$ mV were applied at temperatures between 923–1223 K in a cell-voltage range corresponding to the oxygen pressure range 0.01–0.209 bar O_2. The data were analyzed by a modified version of Equivalent Circuit software [17].

4. Results and discussion

4.1. Diffusion coefficients

Complex impedance representations of experimental data from both methods obtained at high oxygen partial pressures are shown in Fig. 1. Note that the data represent physically different cases. In the conductivity relaxation experiments only changes of conductivity are monitored, so that the resistance of external wiring, assumed constant, is filtered from the data. The impedance data shown can therefore be related directly to finite length diffusion and surface exchange processes of the oxide sample, represented by the circuit elements T and R_s, respectively. In the example shown in Fig. 1a, the resistance R_s is

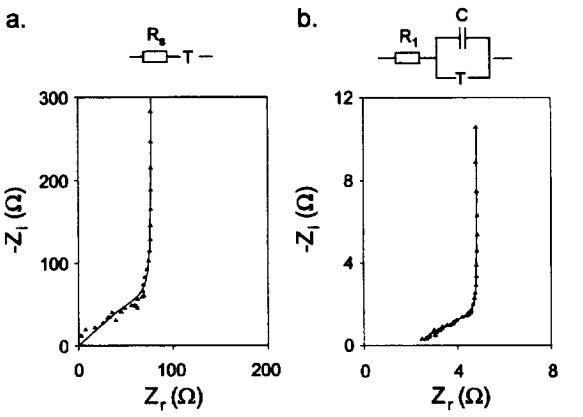

Fig. 1. Impedance representations of experimental data. (a) Conductivity relaxation, $T = 1000$ K, 0.104→0.316 bar O_2; (b) Coulometric titration, $T = 1073$ K, 0.209→0.071 bar O_2. Drawn lines indicate best fits to equivalent circuits shown above.

negligible. A diffusion coefficient $\tilde{D} = 2.8 \times 10^{-6}$ $cm^2\ s^{-1}$ at 1000 K was calculated using Eq. (4) from the best fit.

In the coulometric titration experiments the impedance of the entire cell is measured. Hence, the impedance contains a series resistance associated with external electrical wiring and (possibly) internal gas phase diffusion. Moreover, the gas phase in the cell acts as a capacitance parallel to the impedance of the oxide sample. The corresponding circuit to which the data were fitted is shown in Fig. 1b. R_1 represents the resistance effects such as gas phase diffusion in the bulk and resistance of external wiring. The capacitance C represents the capacitative effect of the gas phase and T is the impedance associated with diffusion in the oxide sample, given by Eq. (6). Best fits to various data indicated that C was proportional to the oxygen pressure, as is expected on theoretical grounds for the gas phase capacitance [14]. In the experiment illustrated in Fig. 1b, C was about 3.2 F. In the same experiment R_1 was about 2.2 Ω, and from the value of T a chemical diffusion coefficient $\tilde{D} = 8.1 \times 10^{-6}$ $cm^2\ s^{-1}$ at 1073 K was calculated using Eq. (6).

Diffusion coefficients were determined with both methods, covering the oxygen partial pressure range 0.03–1 bar O_2. The Arrhenius representations of the diffusion coefficients obtained by both methods are

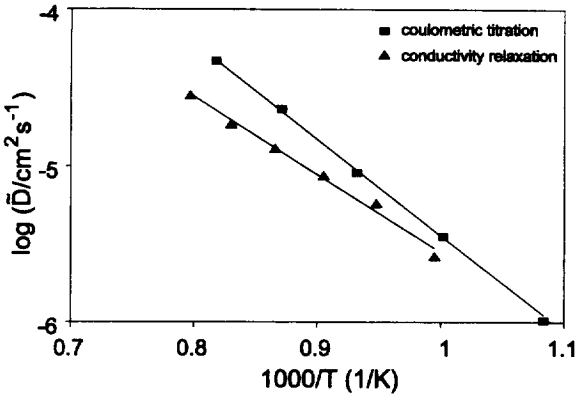

Fig. 2. Chemical diffusion coefficient of oxygen in $La_{0.6}Sr_{0.4}Co_{0.6}Fe_{0.4}O_{3-\delta}$ at 0.1–1 bar O_2 from different relaxation experiments.

Table 1
Self diffusion coefficient (D_O) and vacancy diffusion coefficient (D_V) of oxygen. δ and γ were calculated from Ref. [18].

T(K)	δ	log γ	log(D_O) (cm^2 s^{-1})	log(D_V) (cm^2 s^{-1})
Conductivity relaxation (p_{O_2} = 1 bar)				
1005	0.010	2.51	−8.08	−5.68
1055	0.017	2.35	−7.58	−5.39
1105	0.027	2.24	−7.30	−5.28
1155	0.037	2.15	−7.03	−5.15
1205	0.049	2.04	−6.81	−5.06
1255	0.062	2.00	−6.59	−4.92
Coulometric titration (p_{O_2} = 0.209 bar)				
923	0.007	2.65	−8.64	−6.07
998	0.017	2.37	−7.82	−5.60
1073	0.033	2.19	−7.23	−5.29
1148	0.053	2.08	−6.72	−4.98
1223	0.074	2.02	−6.35	−4.76

shown in Fig. 2. The data points shown are the average values obtained at that temperature. No oxygen pressure dependence was observed within the oxygen partial pressure range in which the chemical diffusion coefficients were determined. The agreement between the two series of data is fairly good. From the results of the conductivity relaxation experiments an activation energy of 95±4 kJ mol^{-1} was calculated for chemical diffusion, while the coulometric titration results yielded 117±5 kJ mol^{-1}. At 1150 K, $\tilde{D}=10^{-5}$ cm^2 s^{-1} was reported for $La_{0.8}Sr_{0.2}Co_{3-\delta}$ [10].

The oxygen deficiency δ, oxygen content c_O ($=3-\delta$) and thermodynamic factor $\gamma=\frac{1}{2}(\partial \ln p_{O_2}/\partial \ln c_O)$ of $La_{0.6}Sr_{0.4}Co_{0.6}Fe_{0.4}O_{3-\delta}$ were calculated at selected temperatures and pressures from oxygen coulometric titration data reported previously [18]. The oxygen self diffusion coefficient D_O and vacancy diffusion coefficient D_V were determined using the relationships $\tilde{D}=D_O\gamma$ and $D_O c_O = D_V\delta$ under the assumption that the value of $\tilde{D}$ could be assigned to the oxygen partial pressures at the end of the experiment. The resulting values are listed in Table 1. The corresponding activation energies for D_O were 140±15 kJ mol^{-1} and 165±12 kJ mol^{-1} derived from conductivity relaxation and coulometric titration results, respectively, and calculation of the activation energy of D_V yielded 69±11 kJ mol^{-1} and 94±6 kJ mol^{-1}, respectively.

4.2. Surface exchange coefficients

In the coulometric titration experiments the value of R_1 was seen to increase strongly with decreasing oxygen partial pressure. At oxygen pressures below 0.05–0.10 bar the diffusion coefficient could no longer be determined due to the high value of R_1. Similar features observed in potentiostatic step experiments on compounds $La_{0.8}Sr_{0.2}CoO_{3-\delta}$ [14] could be explained by the increased contribution from surface exchange in re-equilibration at lower oxygen partial pressures. The surface exchange process was explicitly taken into account in fitting the impedance spectra by placing an extra resistance R_2 in series with the diffusion element T in the circuit shown in Fig. 1b. The value of R_1 appeared to be independent of oxygen pressure, while R_2 increased strongly with decreasing p_{O_2}, i.e., $R_2 \sim p_{O_2}^n$, where $n=0.5$–1. The absence of mass transfer limitation in the gas phase was concluded from the constancy of R_1. No further attempts were made in this paper to derive values of K_{ex} from data of coulometric titration experiments.

In the conductivity relaxation experiments the times needed to re-equilibrate the samples were also seen to increase strongly at lower oxygen partial pressures. The impedance spectra indicated pure resistive behaviour. Since mass transfer limitation in

the gas phase is absent, the re-equilibration process under these conditions can be attributed to slow interfacial exchange of oxygen. At partial pressures below 0.03–0.10 bar O_2, the effect of diffusion could no longer be observed in the experimental impedance spectra. The value of R_s was determined from the low frequency part of the impedance spectra at low oxygen pressures. The surface exchange coefficient K_{ex} was calculated from R_s using Eq. (4). No systematic differences could be observed between the values of K_{ex} obtained from oxidation and reduction runs.

It has been observed that the oxygen permeation rate through $La_{0.6}Sr_{0.4}Co_{0.8}Fe_{0.2}O_{3-\delta}$ membranes [16] was increased significantly upon treatment of the membrane surfaces for several hours in a 2 M nitric acid solution. The XPS spectra [16] indicated that the acid had decomposed the perovskite phase at the surface into the constituent oxides [19]. The effect on the surface exchange rate is shown in Fig. 3. A small but significant increase of the surface exchange coefficients by a factor of 3–5 can be observed with decreasing pH and increasing duration of the treatment. It should be noted that values of $\tilde{D}$ were not influenced by the treatment.

The oxygen pressure dependence of K_{ex} for the different samples does not vary significantly. K_{ex} is roughly proportional to the oxygen partial pressure. This may indicate that the predominant mechanism of exchange does not change upon treatment, although the rate of exchange may be increased by the presence of basic oxides at the surface. It is possible that the main effect of the acid treatment is an increase of the effective surface area on which exchange of oxygen may occur. SEM analysis indicated that the porosity of the surface increased with duration of the treatment. Etching by HNO_3 was seen to take place primarily via the grain boundaries. The sample treated for 18 h showed the surface region to have a large internal porosity of over 30 μm depth.

Arrhenius plots of K_{ex} are shown in Fig. 4. Data were obtained on the sample treated for 18 h in a 2.5 M HNO_3 solution. The activation energy is about 60–70 kJ mol^{-1}. Its value turned out to be independent of oxygen partial pressure, which is taken as a further indication that the predominant mechanism of oxygen exchange does not change with pressure.

The surface exchange coefficient k_O determined from experiments performed in chemical equilibrium, e.g., isotopic exchange experiments, can be calculated from the present data via $k_O = K_{ex}/\gamma$ [12]. The calculated values are given in Fig. 5. Under the conditions covered by the experiments, the value of the thermodynamic enhancement factor γ varies slightly between 90–150. Therefore k_O and K_{ex} have

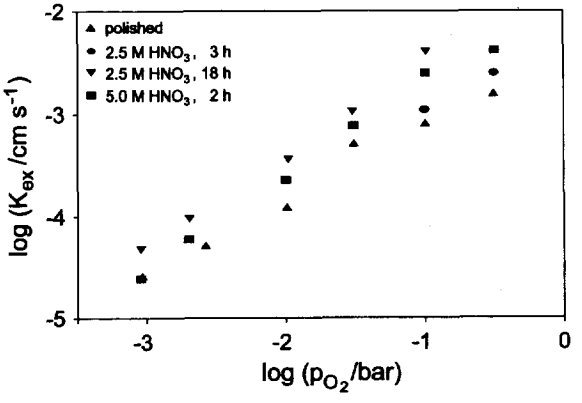

Fig. 3. Influence of acid treatment on magnitude of apparent exchange coefficients K_{ex} at 1225 K.

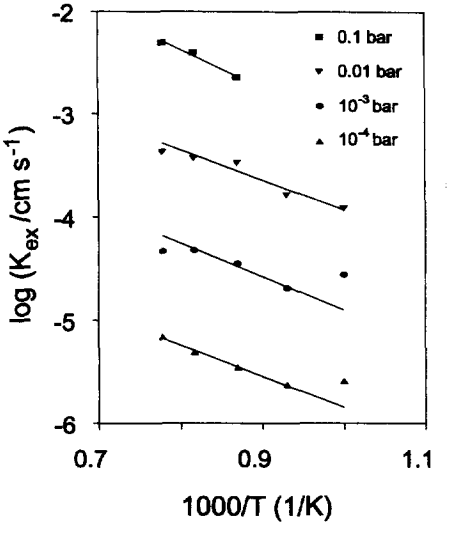

Fig. 4. Arrhenius representations of apparent surface exchange coefficients K_{ex} at different oxygen partial pressures of a sample treated for 18 h in a 2.5 M nitric acid solution.

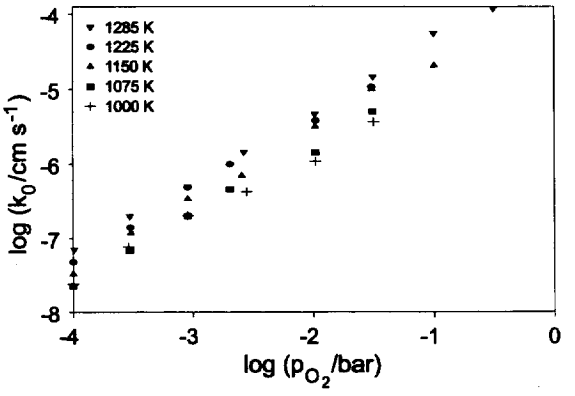

Fig. 5. Surface exchange coefficients k_O of a sample treated for 18 h in a 2.5 M nitric acid solution.

the same activation energy within experimental error. The general trends are similar to those observed previously on $La_{1-x}Sr_xFeO_{3-\delta}$ [12].

The obtained values are close to those of isotopic exchange data reported [1], i.e., $k_O = 2\times10^{-5}$ cm s^{-1} for $La_{0.6}Ca_{0.4}Co_{0.8}Fe_{0.2}O_{3-\delta}$, and $k_O = 5\times10^{-6}$ cm s^{-1} for $La_{0.8}Sr_{0.2}CoO_{3-\delta}$ at 1073 K at high oxygen pressure. The strong oxygen pressure dependence of k_O may indicate that the rate-determining step in the exchange process involves molecular oxygen. In recent conductivity relaxation studies on $La_{1-x}Sr_xFeO_{3-\delta}$ [12] and $La_{1-x}Ca_xCrO_{3-\delta}$ [13] it was possible to correlate the surface exchange coefficients with the concentration of oxygen vacancies in the bulk of the material. In contrast, such a relationship could not be found for the compound under investigation here. It should be noted that the former compounds are p-type semiconductors, while $La_{0.6}Sr_{0.4}Co_{0.6}Fe_{0.4}O_{3-\delta}$ exhibits metallic-like features [18]. It is therefore possible that the rate-determining step is dependent on the electronic structure of the compound.

5. Conclusions

Both the magnitude of the chemical diffusion coefficients $\tilde{D}$ and its activation energy determined from conductivity relaxation and potentiostatic step experiments on samples of 0.5–2.5 mm thickness are found to be in reasonable agreement. In the range 923–1255 K, the chemical diffusion coefficient varies between 10^{-6}–5×10^{-5} cm^2 s^{-1}, corresponding to an activation energy of 90–120 kJ mol^{-1}. The re-equilibration processes at oxygen pressures of 0.1–1 bar is governed by diffusion. At oxygen pressures below 0.01–0.03 bar the re-equilibration process is governed by slow kinetics of interfacial exchange. The surface exchange coefficient K_{ex} is almost proportional to the oxygen partial pressure. The activation energy for K_{ex} is about 60–70 kJ mol^{-1} and is found to be independent of oxygen pressure. Treatment of the oxide surface in a nitric acid solution for several hours does not alter the oxygen pressure dependence, but increases the surface exchange rate with by a factor 3–5. The oxygen pressure dependence of the surface exchange coefficient k_O suggests the involvement of molecular oxygen in the rate-determining step of the surface reaction.

References

[1] S. Carter, A. Selcuk, R.J. Chater, J. Kajda, J.A. Kilner, B.C.H. Steele, Solid State Ionics 53–56 (1992) 597.
[2] I. Yasuda, K. Ogasawara, M. Hishinuma, in: T.A. Ramanarayanan, W.L. Worrell, H.L. Tuller (Eds.), Ionic and Mixed Conducting Oxides, Proceedings of the 2nd International Symposium, The Electrochemical Society, Pennington, NJ, 1994, p. 164.
[3] Ch. Ftikos, S. Carter, B.C.H. Steele, J. Eur. Ceram. Soc. 12 (1993) 79.
[4] O.F. Kononchuk, D.P. Sutija, T. Norby, P. Kofstad, in: M. Dokiya, O. Yamamoto, H. Tagawa, S.C. Singhal (Eds.), Solid oxide fuel cells, Proceedings of the 4th International Symposium, The Electrochemical Society, Pennington, NJ, 1995, p. 395.
[5] T.M. Gür, A. Belzner, R.A. Huggins, J. Membr. Sci. 75 (1992) 151.
[6] K. Nisancioglu, T.M. Gür, Solid State Ionics 72 (1994) 199.
[7] M.H.R. Lankhorst, H.J.M. Bouwmeester, J. Electrochem. Soc. 144 (1997) 1261.
[8] I. Yasuda, M. Hishinuma, J. Solid State Chem. 115 (1995) 152.
[9] I. Yasuda, M. Hishinuma, Solid State Ionics 80 (1995) 141.
[10] Y. Denos, F. Morin, G. Trudel, in: T.A. Ramanarayanan, W.L. Worrell, H.L. Tuller (Eds.), Ionic and mixed conducting oxides, Proceedings of the 2nd International Symposium, The Electrochemical Society, Pennington, NJ, 1994, p. 150.
[11] F. Morin, React. Solids 7 (1989) 307.
[12] J.E. ten Elshof, M.H.R. Lankhorst, H.J.M. Bouwmeester, J. Electrochem. Soc. 144 (1997) 1060.

[13] I. Yasuda, T. Hikita, J. Electrochem. Soc. 141 (1994) 1268.
[14] M.H.R. Lankhorst, Coulometric titration experiments, in: Thermodynamic and transport properties of mixed ionic-electronic conducting perovskite-type oxides, Thesis, University of Twente, Enschede, The Netherlands, 1997.
[15] J.E. ten Elshof, H.J.M. Bouwmeester, H. Verweij, Appl. Catal. A. 130 (1995) 195.
[16] N. Miura, Y. Okamoto, J. Tamaki, K. Morinaga, N. Yamazoe, Solid State Ionics 79 (1995) 195.
[17] B.A. Boukamp, Equivalent Circuit, software, 2nd ed., University of Twente, Enschede, the Netherlands, 1989.
[18] M.H.R. Lankhorst, J.E. ten Elshof, J. Solid State Chem. 130 (1997) 302.
[19] J.E. ten Elshof, H.J.M. Bouwmeester, H. Verweij, Solid State Ionics 89 (1996) 81.